Defect Turbulence in Quasi-2D Creeping Dusty-Plasma Liquids

Wei-Yen Woon and Lin I

Department of Physics, National Central University, Chungli, Taiwan 32054, Republic of China

(Received 14 August 2003; published 12 February 2004)

We report the intermittent and heterogeneous plastic structural rearrangement at the kinetic level in a quasi-2D creeping dusty-plasma Coulomb liquid through directly tracking each particle trajectory and measuring the evolution of each associated local bond-orientational order. The thermal agitation and external shear have comparable strengths. Their interplay with the Coulomb coupling enhances particle hopping, and induces the loss of local structural memory and avalanche-type excitation of topological defect clusters following the universal scaling behaviors of cluster size in *xyt* space, akin to the generic behavior of self-organized criticality. Increasing shear tends to reduce the aspect ratio of the temporal to the spatial spans of the defect cluster in *xyt* space.

DOI: 10.1103/PhysRevLett.92.065003 PACS numbers: 52.27.Lw, 05.40.–a, 05.65.+b

Macroscopically, when a liquid is gently sheared, smooth creeping flow is observed [1]. Down to the kinetic level at the molecular scale, the above smooth picture is complicated by the spatiotemporal heterogeneity induced by the discrete nature and large thermal fluctuations [2]. However, the difficulty of direct visualization under the small molecular scale for liquid in Nature makes it hard to construct the picture beyond the mean field approach. In this report, through directly tracking each particle trajectory and measuring the evolution of the associated structural order, we address experimentally the issue of defect turbulence with microscopic spatiotemporal structural rearrangement using a toy system, the sheared cold quasi-2D dusty-plasma liquid (DPL) confined in a channel.

When a patterned extended system is excited, the ordered structure can be distorted through topological rearrangement. Defect turbulence associated with intermittent and heterogeneous defect fluctuations in patterned nonlinear systems, and defect excitations in creeping *crystals* under external shear serve as good examples [3–6]. Intuitively, this idea is hard to apply for the *microscopic liquid* in which the stochastic thermal agitation makes the system exhibit disordered long term motion and microstructure. However, down to the kinetic level, the mutual interaction is still strong enough to hold the short range spatiotemporal structural correlation. For example, in a cold 2D liquid melted from a triangular lattice, the interparticle distance remains similar and most particles are still surrounded by six nearest neighbors. The thermal motion distorts the local structural order through the formation of topological defects, each with nearest neighbor number deviating from six, around the interface between the defect-free domains with triangular lattice structure [Fig. 1(b)] [7–10]. Namely, under moderate shear which further affects the structural rearrangement, the idea of defect turbulence can be used to characterize the viscoplastic structural organization in a creeping liquid.

From a more general view, the microscopic liquid belongs to the general category of nonlinearly coupled subexcitable systems such as sandpilee systems, earthquake systems, creeping crystals, noise excited chemical systems, etc. [6,10–15]. Despite the seemingly disruptive random effect driven by noise or external drive in these systems, avalanche-type bursts of activities with spatiotemporal correlation take place after slowly accumulating perturbations beyond a local threshold. The excited sites can form clusters with fractal-type structure and a scale-free power law distribution of cluster sizes as described by the SOC (self-organized criticality) model, through spatial coupling and dynamical selections during the cascaded activities of state renewal with the similar physical mechanism. From this point, our study serves as a paradigm at the microscopic level to test the universality of the SOC model for systems driven *simultaneously* by noise and external stress.

Dynamically, in a cold 2D liquid, the stochastic thermal kicks make particles alternately exhibit small amplitude motions in the cages formed by the surrounding particles, or exhibit cooperative fast vortex or string-type

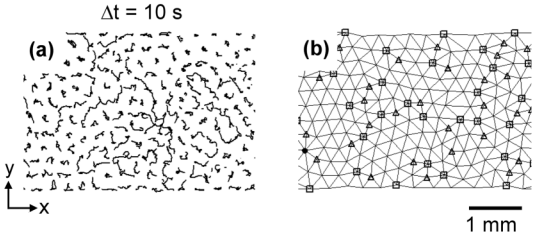

FIG. 1. (a) Typical particle trajectories with 10 sec exposure showing the domain with caged motion surrounded by the hopping strings and vortices for the shear-free run I. (b) One of the corresponding triangulation plots of a snapshot of particle positions showing the formation of defect clusters. The triangles and squares correspond to the −1 (fivefold) and +1 (sevenfold) topological defects, respectively, where the local lattice orientations are distorted.

 0031-9007/04/92(6)/065003(4)$22.50 © 2004 The American Physical Society

hoppings surrounding the temporarily ordered domain [Fig. 1(a)] [9]. Topological defects [e.g., clusters of +1 and −1 disclination defects with seven and five nearest neighbors, respectively; see Fig. 1(b)] forms when the lattice lines are distorted after accumulating sufficient local perturbation [8,9]. The hopping excitation ceases after traveling about one lattice constant, which resettles the distorted local region back to the more ordered defect-free domains [9]. Namely, the stick-slip motions cause the spatiotemporal fluctuations of structural order and the propagation of heterogeneous deformation, associated with the generation, dissociation, propagation, interaction, recombination, and annihilation of defects [8,9].

In a creeping liquid, the external shear further enhances particle motion but it has a different effect from thermal noise. The thermal noise provides spatially and temporally uncorrelated kicks which have uniform spatiotemporal statistical distribution. It either supports or breaks the cascaded spatiotemporal propagation of cooperative defect excitation in *xyt* space as a percolation process after initiating the excitation [15]. However, the external constant shear provides a persistent and directional slow drive along the boundary. It breaks the symmetry, pumps in vorticity, and promotes rotational type hopping mixing which cascades into the interior part through many body interactions [16]. It enhances the viscoplastic structural rearrangement, especially after accumulation over longer time interval. The rearrangement could also be temporarily jammed, if the force chain percolates across the system [17]. Note that unlike in the stressed solid the additional noise perturbation in liquid can unlock the jamming, which leads to the absence of a finite yield stress.

In this study, unlike the creeping crystals or sheared granular systems which have small thermal noise effect [6,17], we investigate the regime where shear has comparable strength to thermal noise. Through tracking the local and global evolution of bond-orientational order (BOO) [7,9], we identify the effect of shear in addition to that of thermal agitation on the spatial and temporal defect fluctuations, after measuring the nonlinear mean responses of defect number density and shear-induced velocity. We also investigate the universal scaling behaviors of spatiotemporal defect excitations.

Dusty-plasma crystal or liquid with sub-mm interparticle spacing can be formed by the suspended micrometer sized particles in low pressure gaseous discharges, through the strong Coulomb coupling induced by the strong negative charging ($\sim 10^4$ electrons per particle) from the background plasma [18–20]. In our experiment, a weakly ionized discharge ($n_e \sim 10^9$ cm^{-3}) is generated in 250 mTorr Ar gas using a 14 MHz rf power system operated at 2.0 W, similar to what was described elsewhere [16]. Two parallel vertical plates 42 mm in length, 14 mm in height, and 12 mm in separation are put on the center region of the bottom electrode surface to confine negatively charged polystyrene particles at 7 μm diameter by the strong electric field in the surrounding dark space (sheath) adjacent to confining walls. Vertically, the suspended dust particles are aligned with eight particles for each chain through the wake field effect of the downward ion flow [16,21]. Particles in the same chain move together horizontally. The mean interchain distance a is 0.3 mm. This quasi-2D liquid has *smooth slipping boundaries*. Two parallel and counterpropagating cw laser sheets (488 nm Ar^+ laser) with 0.4 mm half width and 2.5 mm height (covering the entire vertical chain) are introduced horizontally to push the two outmost rows of particles nearby each boundary. The radiation pressure is proportional to the laser power [16].

The chain positions in the horizontal viewing plane are tracked through digital video microscopy. We identify defects and analyze the dynamics of the structural rearrangement through measuring the evolution of local BOO, $\Psi_6(r) = \frac{1}{N_r}\sum_i \exp(i6\theta_k)$, where θ_k is the angle of the bond from the particle at r to its kth nearest neighbor, and N_r is the number of the nearest neighbors [7,9]. $|\Psi_6| = 1$ at a perfect sixfold lattice site and decreases

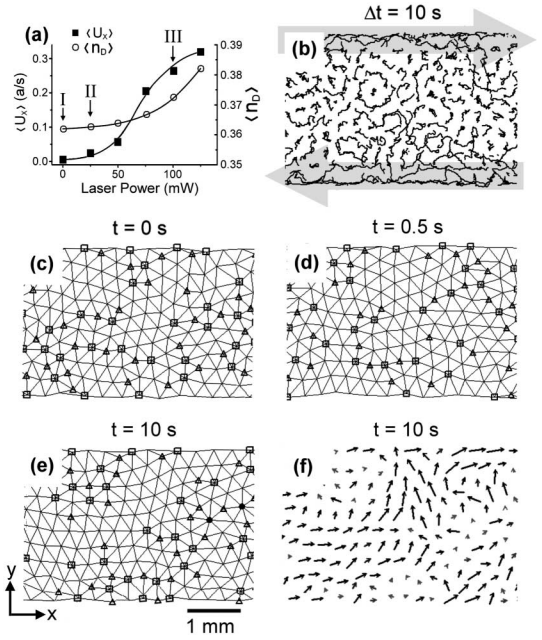

FIG. 2. (a) The nonlinear responses of the mean longitudinal velocity of particles in the laser driven zoom and the mean defect number density (normalized by the total number of particles) to the laser intensity. I, II, and III correspond to the three different runs where the statistical behaviors are measured. (b) Typical particle trajectories with 10 sec exposure showing the stress enhanced motion in run III (especially for the regions nearby the boundaries). The two arrows indicate the positions and directions of the two counterlaser beams. (c)–(e) The corresponding sequential snapshots of defect configuration with different time intervals. In short interval (≤ 1 sec), the cluster configuration only slightly changes. However, it drastically changes after 10 sec. (f) The BOO configuration corresponding to (e). The ordered domain has larger BOO with more coherent alignment.

when the local ordered structure is distorted. A defect site can be treated as an excited site losing local BOO. Moreover, the size distribution of defect clusters in the xyt 3D space is analyzed. The statistics are averaged over 10 000 picture frames.

Figure 2(a) shows the nonlinear increases of the mean longitudinal velocity $\langle U_x \rangle$ of particles at the boundary and the mean defect number density $\langle n_D \rangle$ (averaged over the entire liquid and normalized by the total particle number) with the laser power (note that the thermal speed measured at 10 sec interval is about $0.1a/\text{sec}$). We compare three cases, shear-free (run I), weakly driven (run II, at 25 mW laser power), and more strongly driven (run III, at 100 mW laser power) cases. Figure 2 also shows the typical particle trajectories and the corresponding evolution of defect clusters for run III. In the form of connected dipole ($+1/-1$ defect pair) and sometimes even monopole ($+1$ or -1 defect) defect chains, defects tend to cluster along the interface between the temporary defect-free domains with different bond orientation (BO). Defect configuration changes as time evolves. The shear-induced rotation of bond direction can be more easily observed by tilting the figures and looking at a smaller angle. Besides the defect plots, the corresponding analog measure of the local order Ψ_6 is shown in Fig. 2(f). The angle of each vector shows the local BO, θ_6. The defect sites have small $|\Psi_6|$.

Tracking the temporal evolution of Ψ_6 of each particle characterizes the dynamics of local structural rearrangement. Figure 3(a) shows the typical temporal evolution of $|\Psi_6|$ and the corresponding defect-on/defect-off telegraphlike signals by tracking a single particle sitting $3a$ from the upper boundary. The corresponding trajectories of Ψ_6 in the complex plane shown in Fig. 3(b) further illustrate the evolutions of θ_6 and $|\Psi_6|$. Unlike the thermally excited chaotic excursion with a smaller variation of θ_6 in the shear-free run I, the clustering around $\theta_6 = 3\pi/2$ followed by the more persistent rotation of BO in the shear run III manifests the shear enhanced stick-slip rotation of θ_6 (i.e., vorticity excitation). The temporal correlation of local BOO, $g_6(\tau) = \langle \Psi_6^*(\tau)\Psi_6(0) \rangle$, averaged over all the particles, shows the structural relaxation [Fig. 3(c)]. Figure 3(d) plots the histogram P(T) of the time interval T between two successive local defect excitations in the defect telegraph over all the particles. The stretched exponential distribution manifests the nonrandom nature of the defect excitation [22]. At the small time interval (<1 sec), the moderate shear induces very little motion. The caged thermal motion dominates, which tends to generate short bursts of $+1, -1/-1, +1$ dislocation pairs [compare Figs. 2(c) and 2(d)] [9], and make $P(T)$ nearly independent of the stress intensity at the small T end. At the larger time scale (≥ 1 sec), the shear-induced rotational hopping mixing gradually accumulates and causes the faster descending of $P(T)$ with the increasing shear. The faster change of $|\Psi_6|$ and the faster rotation of BOO more quickly washes out the BOO memory and leads to the faster decay of $g_6(\tau)$ with increasing shear.

The strength of each spatiotemporally correlated structural rearrangement event can be measured by counting N_{Dxyt}, the number of defects in each defect cluster in xyt space. The probability distribution follows $P(N_{Dxyt}) \propto N_{Dxyt}^{-\alpha}$ and $\alpha = 1.6$ for all the cases (Fig. 4). Similar scaling was also found for the size of avalanche excitation in xyt space of a noise driven chemical system [15], the energies released in earthquake [6,13], and defect excitation in creeping ice crystal [6]. It manifests the universal behavior regardless of the detailed difference.

We also measure the averaged aspect ratio (temporal to spatial span) of the defect clusters in xyt space. The inset of Fig. 4 shows the power law relation between the time span ΔT_D and the averaged spatial span $\langle N_{Dxy} \rangle = \langle N_{Dxyt}/\Delta T_D \rangle$ of the clusters at size N_{Dxyt} under different shears. The positive exponent indicates that clusters with the larger spatial span persist longer in time. The lower

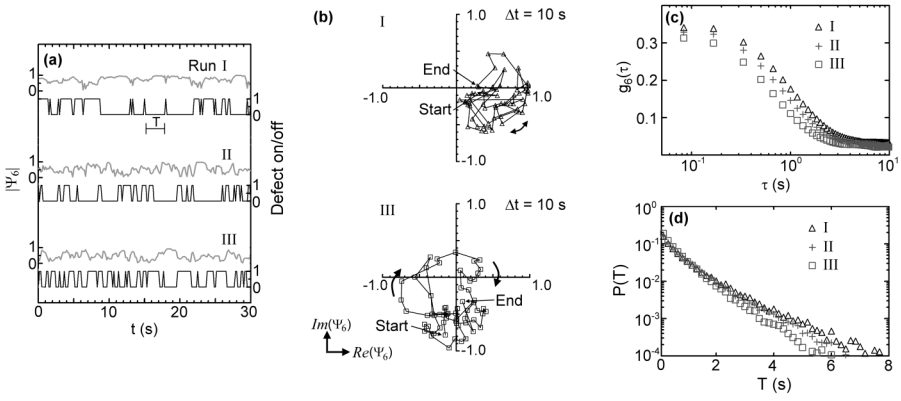

FIG. 3. (a) Gray lines: the typical evolutions of $|\Psi_6|$ of a particle sitting about $3a$ from the upper boundary for runs I, II, and III. Black lines: the corresponding telegraph signals reflecting the evolutions of the defect-on ($=1$) and defect-off ($=0$) states. (b) The corresponding temporal evolution of Ψ_6 at the same sites of runs I and III in the complex plane. The external stress causes the more persistent change of θ_6. The data points are separated by $1/6$ sec interval. (c) The temporal correlation of local BOO, $g_6(\tau)$ of the three runs. (d) The histograms of the time interval T between the two successive defect-on events for the three runs.

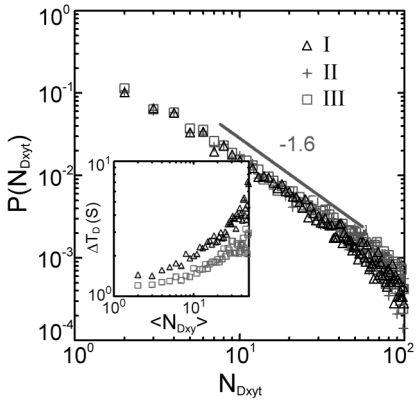

FIG. 4. The histograms of N_{Dxyt} normalized by the total number of clusters in the xyt space for the three runs. The inset shows relation between the temporal span ΔT_D and the averaged spatial span $\langle N_{Dxy} \rangle$ of the defect clusters in xyt space.

curve with the smaller exponent implies that increasing shear tends to generate flatter cluster in xyt space. Namely, it makes the defect cluster more spread in xy space and less persistent in time. Note that this trend is reversed while increasing the temperature for a shear-free liquids.

In the cold 2D liquid, defect excitations are accompanied by the structure distortion due to particle motion while accumulating sufficient constructive perturbation from shear stress and thermal agitation. They aggregate around the boundaries of the temporarily ordered domains to gradually accommodate the mismatch between the different BOO of the adjacent domains. The Coulomb coupling tends to support the collective propagations of perturbations and defects, as well as reforming the ordered triangular structure. After hopping, the more ordered local domain is reformed, in which only short bursts of quadrupole type defect excitations occur under the small lattice distortion induced by caged motion [8]. Comparing to the stochastic thermal drive, the large uniform spatial extension of the directional stress along the system boundary enhances the global vortex mixing assisted by thermal noise, and makes the clusters more plausible to merge into larger clusters in xy space. The persistent drive also continually pumps vorticity into the system [16], promotes the perturbation propagation, and speeds up structural reorganization through more frequent jamming and hopping. It induces faster decay of $g_6(\tau)$, shortens the defect cluster life time, and causes the smaller aspect ratio of the temporal span to the spatial span. The increasing spatial size and the decreasing temporal span leads to the universal scaling of N_{Dxyt} in xyt space regardless of the shear intensity.

In conclusion, we investigate the microscopic defect turbulence associated with the change of structured bond breaking in a creeping Coulomb liquid. The defect bursts with short lifetime are mainly excited by the thermal agitation. The effect of external shear accumulates over longer time scale, which enhances bond rotation and breaking through more frequent hopping and jamming. It leads to the smaller aspect ratio of the temporal to spatial span of the defect cluster in xyt space, which is opposite to the effect of increasing temperature. The scale-free power law distribution of defect cluster size in xyt space manifests that the universal SOC behavior is still obeyed at the microscopic level simultaneously driven by noise and external shear.

This work is supported by the National Science Council of the Republic of China under Contract No. NSC-91-2119-M009-022.

[1] T. E. Faber, *Fluid Dynamics for Physicists* (Cambridge University Press, Cambridge, 1995).
[2] J. Gollub, Phys. Today **56** (1), 10 (2003).
[3] P. Coullet, L. Gil, and J. Lega, Phys. Rev. Lett. **62**, 1619 (1989); K. E. Daniels, and E. Bodenschatz, Phys. Rev. Lett. **88**, 034501 (2002).
[4] D. A. Egolf and H. S. Greenside, Phys. Rev. Lett. **74**, 1751 (1995).
[5] G. D. Granzow and H. Riecke, Phys. Rev. Lett. **87**, 174502 (2001); Y. N. Young and H. Riecke, Phys. Rev. Lett. **90**, 134502 (2003).
[6] M. C. Miguel *et al.*, Nature (London) **410**, 667 (2001); **410**, 667 (2001).
[7] K. J. Strandburg, *Bond-Orientational Order in Condensed Matter Systems* (Springer, New York, 1992).
[8] C. H. Chiang and Lin I, Phys. Rev. Lett., **77**, 647 (1996); Y. J. Lai and Lin I, Phys. Rev. E **64**, 015601(R) (2001).
[9] Y. J. Lai and Lin I, Phys. Rev. Lett., **89**, 155002 (2002).
[10] C. Reichhardt and C. J. O. Reichhardt, Phys. Rev. Lett. **90**, 095504 (2003).
[11] P. Bak, C, Tang, and K. Wiesenfeld, Phys. Rev. Lett. **59**, 381 (1987).
[12] E.g., H. J. Jensen, *Self-Organized Criticality* (Cambridge University Press, Cambridge, 1998).
[13] B. Gutenberg and C. F. Richter, Bull. Seismol. Soc. Am. **34**, 185 (1944).
[14] P. Bak, K. Christensen, H. Danon, and T. Scanlon, Phys. Rev. Lett., **88**, 178501 (2002).
[15] J. Wang, S. Kadar, P. Jung, and K. Showalter, Phys. Rev. Lett., **82**, 855 (1999).
[16] W. T. Juan, M. H. Chen, and Lin I, Phys. Rev. E, **64**, 016402 (2000).
[17] M. E. Cates, J. P. Wittmer, J. P. Bouchaud, and P. Claudin, Phys. Rev. Lett. **81**, 1841 (1998).
[18] J. H. Chu and Lin I, Phys. Rev. Lett. **72**, 4009 (1994).
[19] H. Thomas, *et al.*, Phys. Rev. Lett. **73**, 652 (1994).
[20] Y. Hayashi and K. Tachibana, Jpn. J. Appl. Phys. **33**, L804 (1994).
[21] M. Nambu, S. V. Valdimirov, and P. K. Shukla, Phys. Lett. A **203**, 40 (1995); I. Kourakis and P. K. Shukla, Phys. Lett. A **317**, 156 (2003).
[22] S. N. Majumdar and A. J. Bray, Phys. Rev. Lett. **91**, 030602 (2003).